Journal of Engineering Research and Education
Volume 17, 2025 [195-203]

500 kHz Zero Voltage Switching (ZVS) of Class E Inductive Power Transfer (IPT)-based for Toy Drone Charging System

Syahmi Syafiq Ishak [1], Norezmi Jamal[1*], Farahiyah Mustafa[1], Omar Abu Hassan[1], Norain Sahari[1], Wahab, Nurul Husna Abd[2], Shakir Saat[3], and Huzaimah Husin[3]

[1]Faculty of Engineering Technology, Universiti Tun Hussein Onn Malaysia, Pagoh Campus, 84600 Pagoh, Johor, Malaysia
[2] Faculty of Electrical Engineering & Technology, Universiti Malaysia Perlis, Pauh Putra Campus, 02600 Arau, Perlis, Malaysia
[3]Advanced Sensors & Embedded Control System (ASECs) Research Group, Faculty of Electronics and Computer Engineering and Technology, Universiti Teknikal Malaysia Melaka, 76100 Durian Tunggal, Melaka, Malaysia

ABSTRACT

This paper comprehensively studies an inductive power transfer (IPT) -based toy drone charging system. The main issue of toy drones are limited flight time and battery capacity. Due to this, it has motivated us to propose a portable charging system to power up the battery of a toy drone wirelessly. The Class-E circuit is designed with a single-power MOSFET switch and load network to efficiently drive high-frequency alternating current (AC) with minimal switching losses. Utilizing an Arduino board to generate a pulse width modulation (PWM) switching signal, the impact of the PWM device on the Class-E circuit's switching performance at 500 kHz was explored. The analysis encompasses the performance of the Class-E circuit in terms of Zero Voltage Switching (ZVS) and output load. The findings revealed that the PWM waveform from Arduino achieves an approximately 50% duty cycle and enables optimal ZVS of the Class-E circuit. Consequently, the MOSFET is activated during the minimum voltage across its drain and source, thereby minimizing switching losses. As a result, the potential application of a Class-E circuit in energizing the transmitter coil for the toy drone was observed.

Keywords: Toy drone; IPT system; ZVS soft switching; Class E circuit

1. INTRODUCTION

Toy drones are getting more diverse and user-friendly, indicating an increase in popularity. They are used for enjoyable activities such as flying in parks, capturing pictures, and racing competitions for entertainment. On the other hand, drones also are widely used in civil and agriculture areas [1]. However, the present problem with toy drones or any other drone type is that they have limited flight time and battery capacity [2]. This is because the battery drains quickly, especially while the battery is at full output power. Consequently, the user needs to recharge the battery by removing the battery from the drone. Due to this, it has motivated us to propose a portable charging system to power up the battery of a toy drone wirelessly. An inductive link is a suitable alternative to transferring electricity at close range without the inconvenience of using a wire to recharge the battery. To energize inductive links and receive enough output power, powerful power electronics circuits are required to be designed either at transmitter or receiver side of Inductive Power Transfer (IPT) system. An inverter is a crucial power electronic circuit that efficiently converts the direct current (DC) electricity generated by solar panels or DC input supply into alternating current (AC) electricity. It has been widely used due to the increasing demand for the use of solar panels to power up the AC load [3].

*norezmi@uthm.edu.my

The different types of inverters, including single inverters, dual inverters, and multi-level inverters, serve similar functions but have distinct characteristics. These characteristics depend on the number and configuration of power switch components used in each type of inverter. H-bridge of full-bridge topology circuit is one of the multilevel inverters, which was famously used in high-power applications [4-6]. For example, a novel push–pull parallel resonant converter-based using four power switches for IPT-based electric vehicle system with 3.3 kW and 86 kHz was proposed by Zhao *et al*., [7]. Next, in drone charging application, Obayashi *et al*., [8] used full-bridge inverter to drive inductive links at 750 W and 85 kHz.

However, the use of multiple switching devices comes with a few drawbacks, such as power losses and complex switching control strategy. Consequently, various authors have conducted studies and made modifications to the H-bridge circuit for photovoltaic system applications, considering different output power levels and load conditions [9-11]. The H-bridge topology experiences efficiency losses and requires complex switching control due to its design involving multiple switching elements. In contrast, a few researchers used dual power switches and single power switch while driving inductive links. For example, Jawad *et al*., [12] used two power switch transistors to drive inductive links in drone charging application.

On the other hand, Ma *et al*., [13] stated that the Class E circuit presents a more favorable alternative with a single power switch in high frequency inverter, resulting in reduced switching losses and simplified control, making it an advantageous choice for DC to AC power converter application. Moreover, it is based on Zero Voltage Switching (ZVS) condition [13]. It has a proven track record in biomedical implant applications [14-15], drone applications [16-17] and solar panel [18]. However, resonant converter has significant drawbacks, including the necessity for a bulk inductor, large Electromagnetic Interference (EMI) filters, high voltage stress on switches, and the challenging design of the gate driver [19].

On top of that, it motivated us to design Class E circuit for toy drone charging system, specifically focused on Class E circuit analysis on the effect of Zero Voltage Switching (ZVS) and inductive links voltage. Thus, this paper is organized by starting with background and literature review. Then, project methodology is discussed in Section 2. Next, experimental results are presented in Section 3. Lastly, the paper will be concluded in Section 4.

2. METHODOLOGY

This section presents the Class E circuit's design through simulation and experimental works as illustrated in Figure 1. The parameter determination was done by theoretical formula [20] and summarized in Table 1. Then, the circuit was simulated using LT Spice software to observe ZVS performance. After the circuit simulation was satisfying, a Class E circuit was constructed and a Rigol oscilloscope was used to acquire the waveform signal during experimental work. The parameter specifications are shown in Table 1.

The LTspice simulation model was used to validate the theoretical calculation. All the passive components were connected to form a simple Class E circuit as illustrated in Figure 2 with the value of parameters as shown in Table 1. IRF510 MOSFET was used to switch correctly. Whenever a MOSFET has been triggered, the choke inductor is more conductive, and the voltage across the shunt capacitor, Cshunt is zero. The shunt capacitor, Cshunt stores the charge after MOSFET is active. The ZVS and load voltage waveform were observed by simulating with 500 kHz frequency, 12 V input voltage, 10 W maximum output power, and the duty cycle is 50%

Table 1 Parameter specifications

Parameters	Values
Operating Frequency, f_o	500 kHz
Input DC supply, V_{dc}	12.0V
Choke Inductor, L_{choke}	26.0 µH
Shunt Capacitor, C_{shunt}	10.0 nF
Series Capacitor, C_{series}	4.0 nF
Series Inductance, L_{series}	30.0 µH
Load Resistance, R_L	10Ω

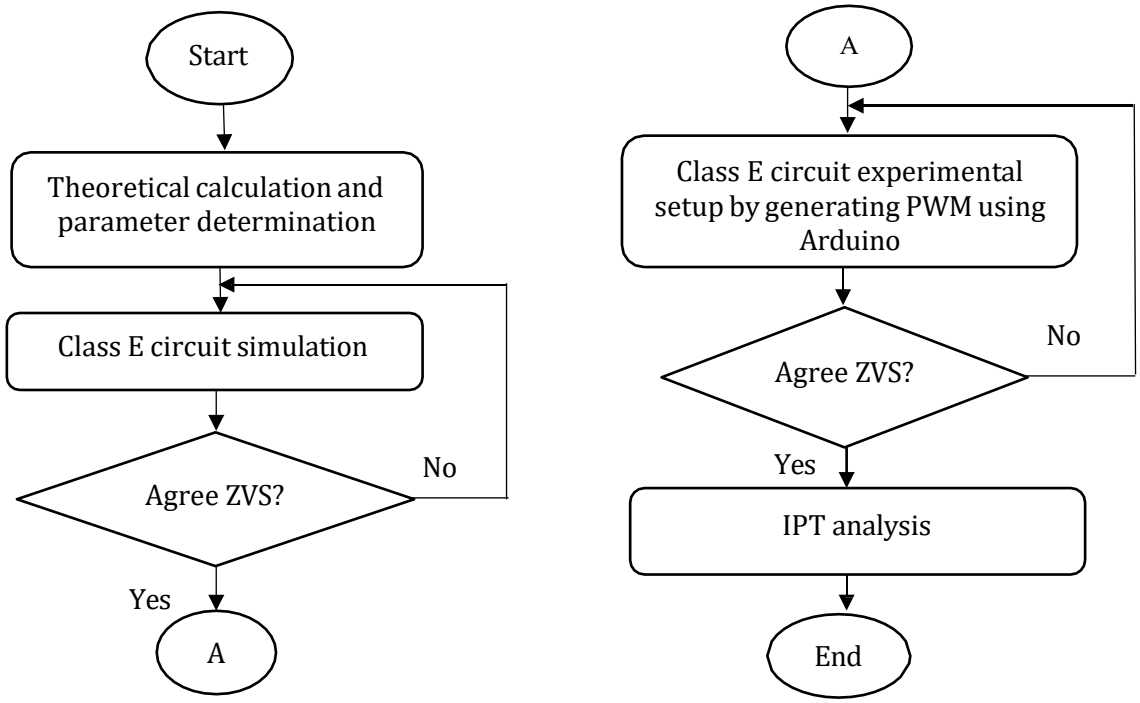

Figure 1. Project methodology overview

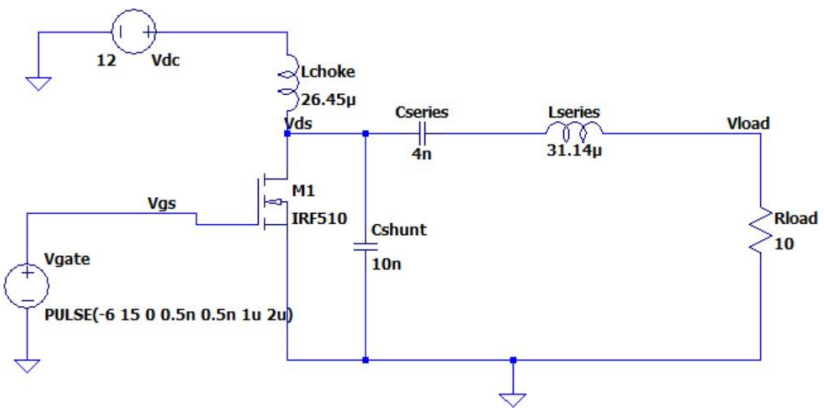

Figure 2. Class E circuit simulation

Next, Class E circuit experimental work was carried out to verify the simulation result. The circuit was constructed based on theoretical circuit calculation and simulation work. Figure 3 depicts the hardware implementation for the Class E circuit. It consists of an Arduino board, TC 4422 gate driver, and a Class E circuit. Arduino board was mainly used to produce a Pulse Width Modulation (PWM) with a periodic square waveform of 500 kHz switching frequency and 12V direct current input supply. Then, the gate driver was required to allow the low current from the Arduino board output signal to drive a MOSFET gate by switching on/off. The current from the driver will charge the gate of parasitic capacitance and correspond to the turn-on time of MOSFET. It is high enough to produce a low drain-source resistance, $R_{ds(on)}$ when MOSFET is turned on.

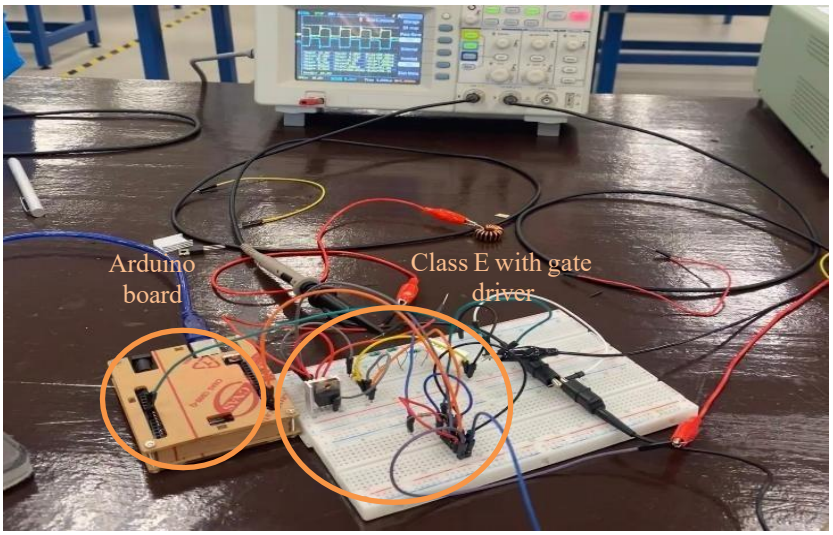

Figure 3. Class E circuit hardware construction

In order to trigger MOSFET gate of Class E resonant converter circuit, 50% duty cycle of square wave signals is required, which was produced by the Arduino board. It was connected before the gate driver to the gate of MOSFET. Next, the circuit was integrated with inductive links for misalignment test and gap analysis as illustrated in Figure 4 and Figure 5, respectively. Lastly, the circuit was tested with a charging system as shown in Figure 6.

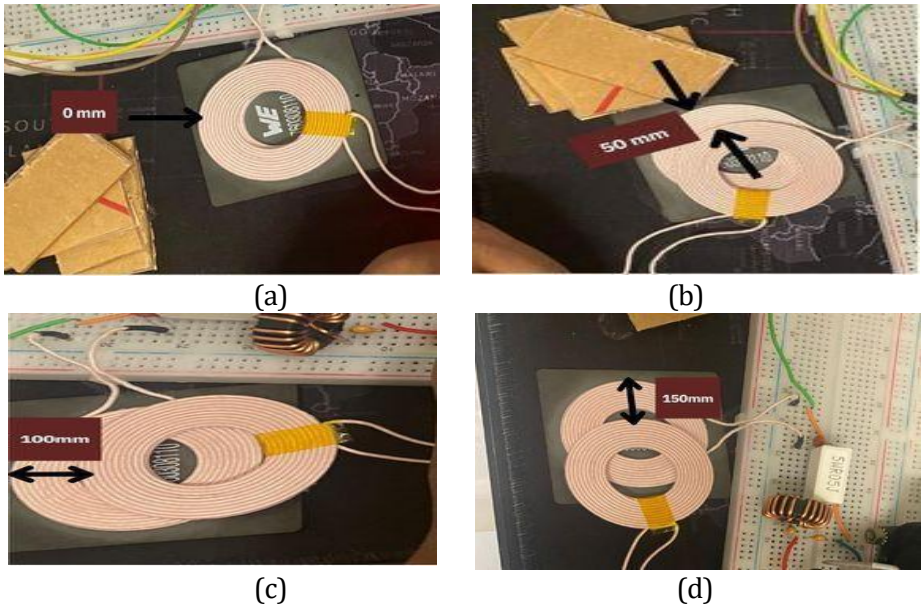

Figure 4. Misalignment test (a) 0 mm (b) 50 mm (c) 100 mm (d) 150 mm

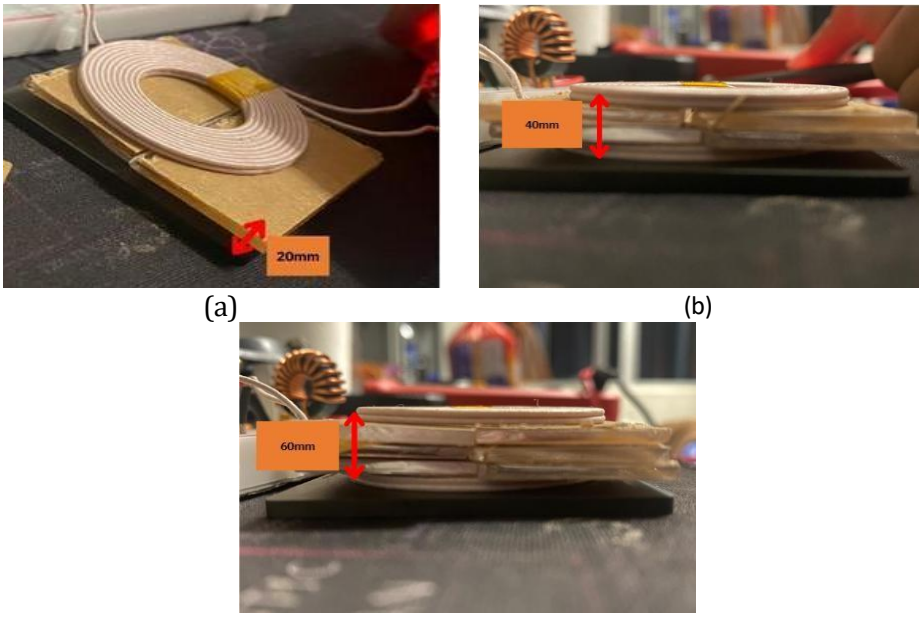

(a) (b)

(c)

Figure 5. Gap analysis (a) 20 mm (b) 40 mm (c) 60 mm

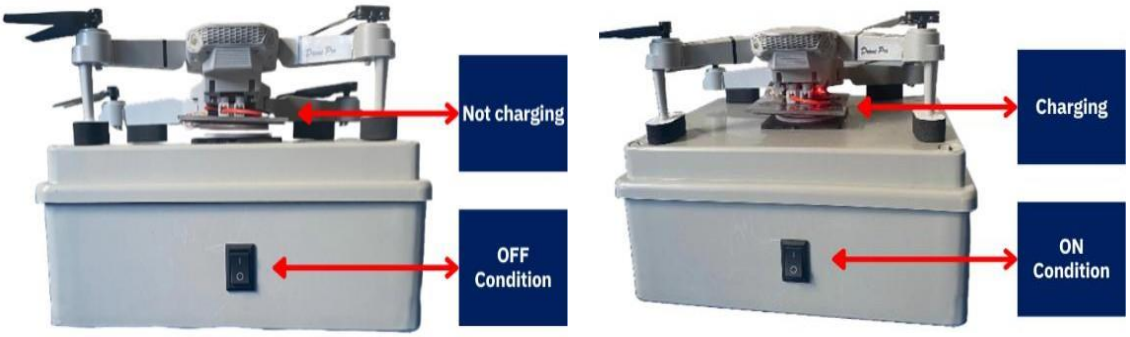

(a) (b)

Figure 6. Circuit packaging for toy drone charging system (a) Switch off condition (b) Switch on condition

3. RESULTS AND DISCUSSION

As illustrated in Figure 7, the voltage across the MOSFET and the shunt capacitance is zero when the MOSFET is turned on. Otherwise, it can be observed that the drain-to-source voltage (V_{ds}) is approximately 36.0 V_{peak} for simulation and 39.2 V for experimental work with a resistive load of 10 Ω during MOSFET is turned OFF. This value is about 3.0 times greater than the value of V_{DD}, which is due to the increase in the charge stored in the shunt capacitor, C_{shunt} for both scenarios. Noted that during simulation work as shown in Figure 7 (a), the transition is set to 2 μs for the switching period. Additionally, the square waveform, which represents the gate-to-source voltage (V_{gs}), is 21.0 V_{p-p} for simulation, while the experimental work depicts 20.8 V_{p-p}.

While in practical work, the MOSFET gate source is powered by Arduino and passed by the MOSFET driver. This is because, without the MOSFET driver, the MOSFET itself cannot be triggered. After the use of the MOSFET driver, the waveform of the Class-E circuit achieved zero voltage switching (ZVS), as shown in Figure 7(b). This is because the MOSFET drivers are

designed to provide rapid switching transitions, which is crucial for achieving ZVS. Without a driver, the gate of the MOSFET might not charge or discharge quickly enough, resulting in non-zero voltage during switching events.

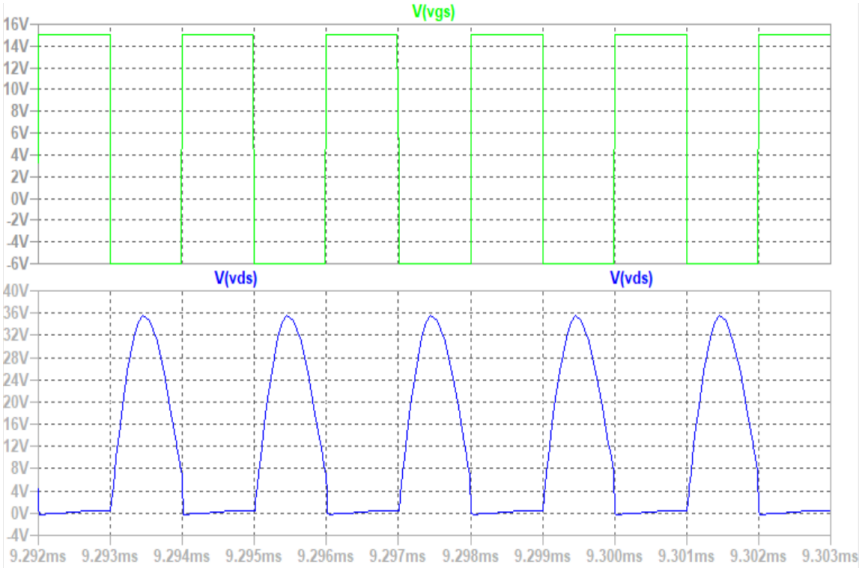

(a)

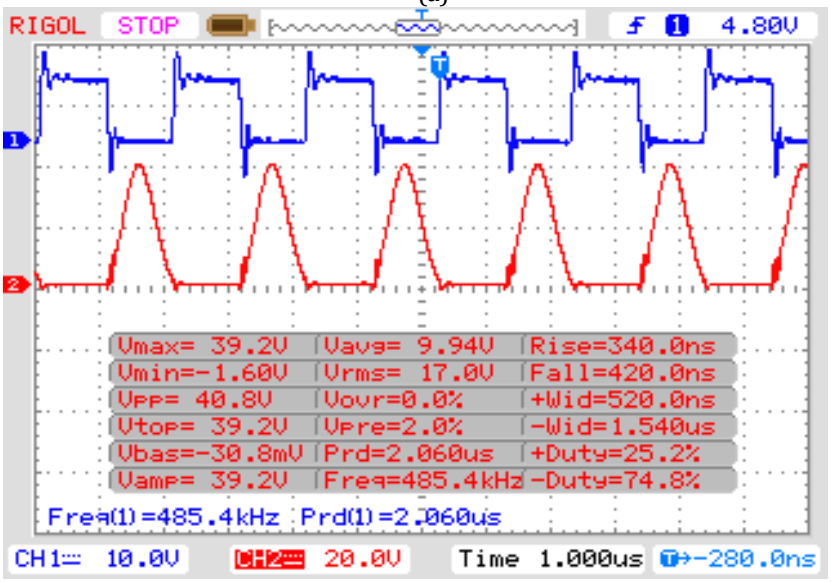

(b)

Figure 7. ZVS of 500 kHz Class E circuit (a) Simulation result (b) Experimental result

Table 2 Performance results

	Simulation	Hardware
Switching frequency, *f* (kHz)	500	485
Voltage drain to source, V_{ds} (V)	36	40.8
Voltage gate to source, V_{gs} (V)	20.8	21
Peak-peak Voltage across transmitter coil, V_1 (V)	9.0	47.2
Peak-peak Voltage across receiver coil, V_2 (V)	3.0	8.4

The voltage across inductive links for simulation and experimental works are illustrated in the Figure 8. The simulated results showed a smoothly sinusoidal waveform of 5 V_p at transmitter side. The sinusoidal waveform for experimental results has some ringing due to leakage

inductance. To ensure the smooth sinusoidal voltage waveform of inductive links, the resonant capacitor has been connected in series at transmitter side.

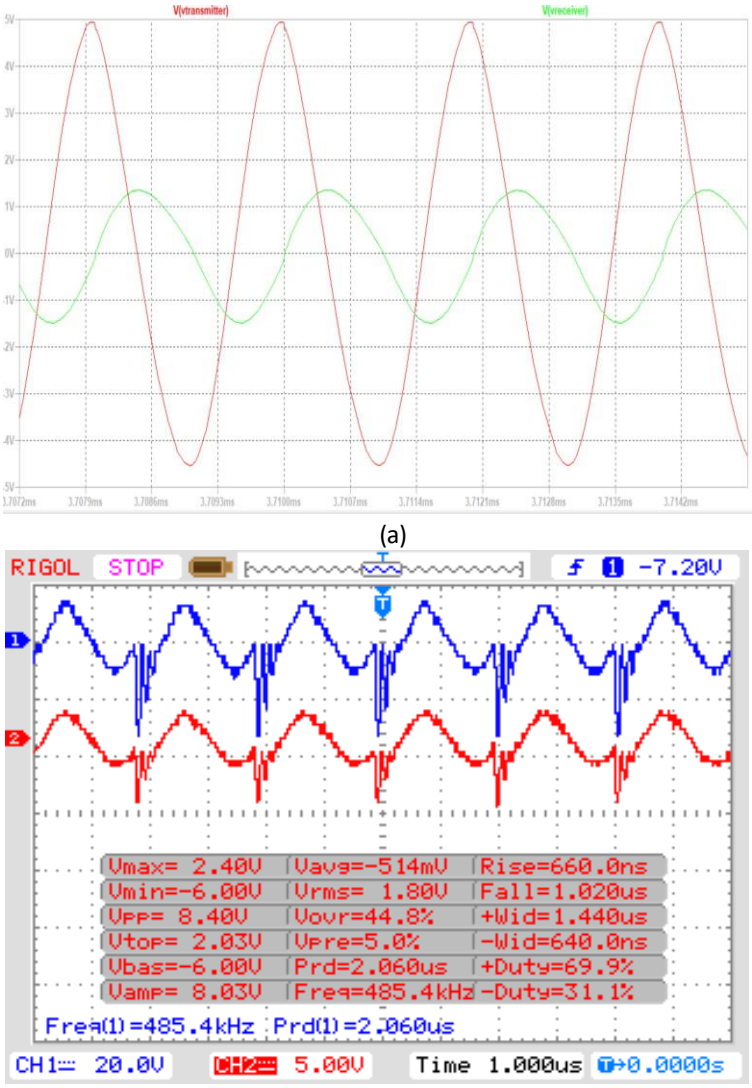

Figure 8. Voltage waveform across inductive links (a) Simulation result (b) Experimental result

Next, Figure 9 (a) shows the air gap test measures how the distance between the transmitter and receiver coils affects the voltage output. The data shows that the output voltage remains relatively stable at 4.49 V and 4.47 V for air gaps of 0 mm and 20 mm, respectively. This stability indicates that the system can handle small air gaps without significant loss in power transfer efficiency. However, as the air gap increases to 40 mm, the voltage drops to 3.85 V, and further to 3.2 V at 60 mm. This gradual reduction is due to the decreased coupling coefficient between the coils, leading to reduced efficiency in power transfer. At an 80 mm air gap, the voltage drops to 0 V, signifying a complete failure in power transfer due to the loss of effective magnetic coupling.

While Figure 9 (b) illustrates the misalignment test assesses the impact of lateral displacement between the transmitter and receiver coils on the voltage output. Initially, the output voltage shows a slight decrease from 4.49 V to 4.04 V when the misalignment increases from 0 mm to 50 mm, demonstrating the system's tolerance to small misalignments. However, as the misalignment grows to 100 mm, the voltage output decreases to 3.633 V, indicating reduced power transfer efficiency. At 150 mm, the voltage sharply drops to 0.0162 V, showing a substantial loss in efficiency due to significant misalignment and minimal magnetic coupling. Finally, at 200 mm

misalignment, the voltage output reaches 0 V, indicating a complete failure in power transfer, as the coils are too far apart laterally to couple effectively.

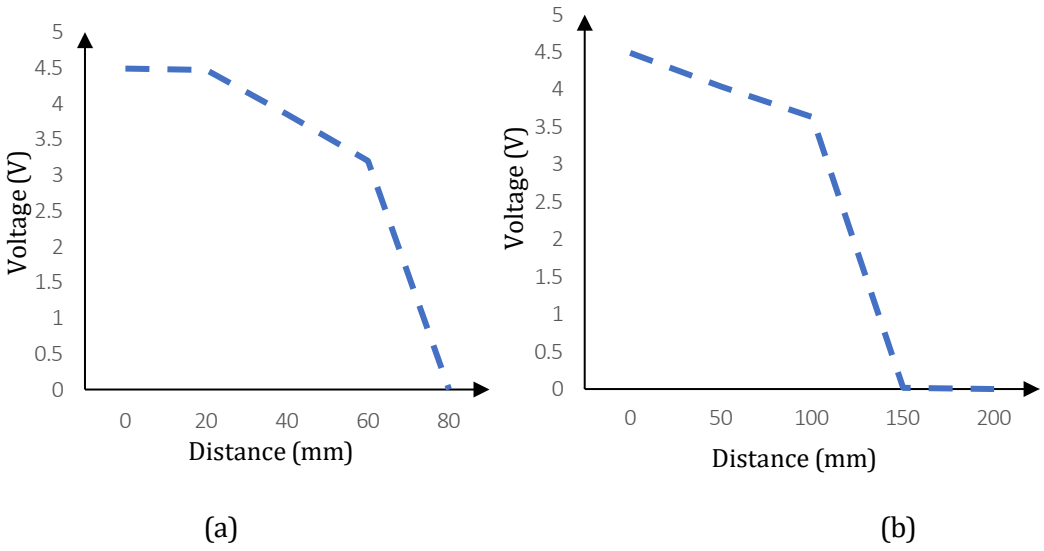

Figure 9. Performance of the induced voltage (a) Air gap test (b) Misalignment test

4. CONCLUSION

Class E circuit has been successfully examined through simulation and experimental results. A PWM signal from an Arduino board controlled the power MOSFET, achieving a 50% duty cycle and 500 kHz frequency. Results showed that zero voltage switching (ZVS) was possible in both simulation and experimental setups, but the hardware implementation had a lower switching frequency than the simulation. Additionally, the achieved findings also highlight the limitations of the system regarding maximum air gap and misalignment tolerances, which are crucial considerations for designing robust and efficient IPT system. Therefore, the rectifier and boosting circuit should be considered for the future development of the receiver circuit to improve the charging time and increase output current.

ACKNOWLEDGEMENTS

Sincerely to express the appreciation to Universiti Tun Hussein Onn Malaysia (UTHM) for providing the facilities to carry out the experimental works.

REFERENCES

[1] Rabiu, L., Ahmad, A., & Gohari, A. (2024). Advancements of Unmanned Aerial Vehicle Technology in the Realm of Applied Sciences and Engineering: A Review. Journal of Advanced Research in Applied Sciences and Engineering Technology, 40(2), 74-95.

[2] Wu, M., Su, L., Chen, J., Duan, X., Wu, D., Cheng, Y., & Jiang, Y. (2022). Development and prospect of wireless power transfer technology used to power unmanned aerial vehicle. Electronics, 11(15), 2297.

[3] Dogga, R., & Pathak, M. K. (2019). Recent trends in solar PV inverter topologies. Solar Energy, 183, 57-73.

[4] Kumar, C. S., & Kalyani, S. T. (2023). Improvement of power quality in smart grid connected pv system using multilevel inverter. Journal of Advanced Research in Applied Sciences and Engineering Technology, 31(1), 1-13.

[5] Maheswari, K. T., Bharanikumar, R., Arjun, V., Amrish, R., & Bhuvanesh, M. (2021). A comprehensive review on cascaded H-bridge multilevel inverter for medium voltage high power applications. Materials Today: Proceedings, 45, 2666-2670.

[6] Kim, J. H., Lee, B. S., Lee, J. H., Lee, S. H., Park, C. B., Jung, S. M., ... & Baek, J. (2015). Development of 1-MW inductive power transfer system for a high-speed train. IEEE Transactions on Industrial Electronics, 62(10), 6242-6250.

[7] Zhao, L., Thrimawithana, D. J., Madawala, U. K., & Hu, A. P. (2019). A push–pull parallel resonant converter-based bidirectional IPT system. IEEE Transactions on Power Electronics, 35(3), 2659-2667.

[8] Obayashi, S., Kanekiyo, Y., Sugaki, K., Watabe, A., Nakakoji, H., Ichikawa, H., & Takao, N. (2022, July). 750-W 85-kHz inductive rapid charging system for mid-sized UAV. In 2022 Wireless Power Week (WPW) (pp. 605-609). IEEE.

[9] Bertin, T., Despesse, G., & Thomas, R. (2023). Comparison between a Cascaded H-Bridge and a Conventional H-Bridge for a 5-kW Grid-Tied Solar Inverter. Electronics, 12(8), 1929.

[10] Charan, N. H., Bandyopadhyay, A., & Guerrero, J. M. (2023). Performance evaluation of single-phase boost-type cascaded H-bridge inverter in the applications of grid-tied photovoltaic systems. IEEE Journal of Emerging and Selected Topics in Power Electronics, 12(2), 1416-1426.

[11] Shuvo, S., Hossain, E., Islam, T., Akib, A., Padmanaban, S., & Khan, M. Z. R. (2019). Design and hardware implementation considerations of modified multilevel cascaded H-bridge inverter for photovoltaic system. Ieee Access, 7, 16504-16524.

[12] Jawad, A. M., Jawad, H. M., Nordin, R., Gharghan, S. K., Abdullah, N. F., & Abu-Alshaeer, M. J. (2019). Wireless power transfer with magnetic resonator coupling and sleep/active strategy for a drone charging station in smart agriculture. IEEE Access, 7, 139839-139851.

[13] Ma, J., Wei, X., Nguyen, K., & Sekiya, H. (2020). Analysis and design of generalized class-E/F 2 and class-E/F 3 inverters. IEEE Access, 8, 61277-61288.

[14] Ahmadi, M. M., Pezeshkpour, S., & Kabirkhoo, Z. (2021). A high-efficiency ASK-modulated class-E power and data transmitter for medical implants. IEEE Transactions on Power Electronics, 37(1), 1090-1101.

[15] van Nunen, T. P., Mestrom, R. M., & Visser, H. J. (2023). Wireless power transfer to biomedical implants using a class-e inverter and a Class-DE rectifier. IEEE Journal of Electromagnetics, RF and Microwaves in Medicine and Biology, 7(3), 202-209.

[16] Hasan, K. K., Saat, S., Yusop, Y., & Awal, M. R. (2022). Development of self-charging unmanned aerial vehicle system using inductive approach. International Journal of Power Electronics and Drive Systems, 13(3), 1635.

[17] Jawad, A. M., Nordin, R., Jawad, H. M., Gharghan, S. K., Abu-Samah, A., Abu-Alshaeer, M. J., & Abdullah, N. F. (2022). Wireless drone charging station using class-E power amplifier in vertical alignment and lateral misalignment conditions. Energies, 15(4), 1298.

[18] Karafil, A. (2023). Thinned-out controlled IC MPPT algorithm for class E resonant inverter with PV system. Ain Shams Engineering Journal, 14(5), 101992.

[19] Chen, S., Chen, Y., Zhang, B., & Qiu, D. (2022). Very-high-frequency resonant boost converter with wide output power range and synchronous drive. IEEE Transactions on Industrial Electronics, 70(9), 8928-8938.

[20] Yusmarnita, Y., Saat, S., Hamidon, A. H., Husin, H., Jamal, N., Kh, Kamarudin., & Nguang, S. K. (2015). Design and analysis of 1MHz class-E power amplifier. WSEAS Journal, 14.